リーダー細胞に誘導される集団細胞回転

松下勝義, 薮中俊介 [A], 橋村秀典 [B], 桑山秀一 [C], 藤本仰一

阪大院理 生物, [A] 九大院理 物理, [B] 東大総合文化 相関基礎, [C] 筑波大 生命環境

概要

生物系においては細胞の集団での回転運動がしばしば現れる. 我々はこれらの回転運動の誘導要因がリーダー細胞である可能性について調べた. この目的の下, 我々はリーダー細胞が異種分子細胞間接着に持続的な極性を持つことを仮定し, 細胞 Potts 模型を基に集団細胞回転運動の模型を構成した. そして, リーダー細胞がこの回転運動を誘導する可能性を示した.

Leader-guiding collective cell rotation

Katsuyoshi Matsushita, Sunsuke Yabunaka[A], Hidenori Hashimura[B],
Hidekazu Kuwayama[C], and Koichi Fujimoto

Department of Biological Science, Graduate School of Science, Osaka University.
[A]Department of Physics, Graduate School of Science, Kyushu University.
[B]Department of Basic science, Graduate School of Arts and Sciences, The University of Tokyo.
[C]Faculty of Life and Environmental Sciences, University of Tsukuba.

Abstract

In biological systems, collective rotations frequently appear in cell aggregations. We examine leader cells as a possible guide for these collective rotations. For this purpose, we model the multicellular system based on the cellular Potts model for these rotations by assuming the persistently-polarized heterophilic cell-cell adhesion of leader cells. We show a possibility that the leaders guide these rotations.

1 Introduction

In developmental processes in biological systems, eukaryotic cells collectively and spontaneously move to their suitable positions for their fates [1]. One of the spontaneous collective movements is a persistent collective rotation of cell aggregations [2–4]. For example, this rotation sorts out *Dictyostelium discoideum* cells by their fates [3, 5]. This rotation has been investigated by biologists and its guiding mechanisms were speculated to be chemotaxis [6, 7] and molecular chirality [8]. In addition to these mechanisms, the persistence of the rotation lets us deduce the persistent motility in individual cells [9, 10]. This rotation, however, is naively contradictory to the persistent motility, because the persistent motility seems to stabilize only the unidirectional order of movements instead of the rotation [11–15]. Therefore, improvements for matching these mechanisms to the persistence is necessary for the understanding of the collective cell rotations.

As such an improvement, the contact following was theoretically considered and successfully reproduced the rotation [6,7,16,17]. Because the contact following is implemented by the Vicsek-like interaction based on visual recognition [18], it is not simply supposed for natural cells in contrast to birds or fishes. As an alternative improvement independent of such recognition, we focus on the effects of the leader cells which drag the surrounding cells [19]. Namely, we hypothesize that the leader cells guide the rotation. In this case, only the leader cells have the persistent motility, while the surrounding cells do not. Hereinafter, we call the surrounding cells follower cells for convenience in explanation. This hypothesis is based on the fact that leader cells cannot stabilize the unidirectional order in their low concentrations below a certain threshold value necessary for the order.

In the present work, to examine this hypothesis, we model these leading and follower cells based on the cellular Potts model [19, 20]. As a test case of this hypothesis, we consider a persistent motility due to the persistently-polarized heterophilic cell-cell adhesion between leader and follower cells [21] for tractability in this model. By this model, we confirm that the leaders successfully guide these rotations by avoiding the unidirectional order in the case of a few leaders.

2 Model

For our purpose, this work utilizes the two-dimensional cellular Potts model. In this model, cell configurations are represented as Potts states

$m(\boldsymbol{r})$'s. Here, $\boldsymbol{r}$ is a coordinate in a square lattice with linear dimensions of L. $m(\boldsymbol{r})$ takes a number in $\{0, 1, 2, \ldots, N\}$. $m(\boldsymbol{r})$ is the cell index occupying $\boldsymbol{r}$ except for $m(\boldsymbol{r}) = 0$, which is no cell at $\boldsymbol{r}$. The fixed number N is the number of cells. These cells belong to two types of cells with $\tau(m) = 1$ and 2. $\tau(m) = 1$ indicates that the mth cell is a leader cell with a polarity vector $\boldsymbol{p}_m$ and $\tau(m) = 2$ indicates that the mth cell is an unpolarized cell. We additionally set $\tau(0) = 0$. By sampling the consecutive series of these Potts states with Monte Carlo simulation, we simulate the cellular dynamics.

For this simulation, the realization probability for each Potts state is given by the Boltzmann weight $\exp(-\beta\mathcal{H})$. Here, $\mathcal{H}$ is Hamiltonian,

$$\mathcal{H} = \sum_\tau \mathcal{H}_S^\tau + \mathcal{H}_A + \mathcal{H}_B, \qquad (1)$$

and β is an inverse temperature.

The first term in the RHS of Eq. (1) is the surface term

$$\mathcal{H}_S^{\tau'} = \gamma_C^{\tau'} \sum_{\boldsymbol{rr}'} \delta_{\tau'\tau(m(\boldsymbol{r}))}\delta_{\tau'\tau(m(\boldsymbol{r}'))}\eta_{m(\boldsymbol{r})m(\boldsymbol{r}')}$$
$$+ \gamma_E^{\tau'} \sum_{\boldsymbol{rr}'} \eta_{m(\boldsymbol{r})m(\boldsymbol{r}')} \big[\delta_{\tau'\tau(m(\boldsymbol{r}))}\delta_{0m(\boldsymbol{r}')}$$
$$+ \delta_{m(\boldsymbol{r})0}\delta_{\tau'\tau(m(\boldsymbol{r}'))} \big], \qquad (2)$$

where γ_C^τ is the surface tension of cellular interfaces for type τ, γ_E^τ is that between cells with type τ and the empty space. η_{nm} is $1 - \delta_{nm}$ and δ_{nm} is the Kronecker δ. The summation between $\boldsymbol{r}$ and $\boldsymbol{r}'$ is taken over the nearest and next nearest pairs. This summation rule is commonly applied hereinafter.

The second term in the RHS of Eq. (1) is an additional surface term [21],

$$\mathcal{H}_A = \sum_{\boldsymbol{rr}'} \eta_{\tau(m(\boldsymbol{r}))\tau(m(\boldsymbol{r}'))}\eta_{\tau(m(\boldsymbol{r}))0}\eta_{\tau'(m(\boldsymbol{r}))0}$$
$$\times \big[\gamma_H - \gamma_p \big(\boldsymbol{p}_{m(\boldsymbol{r})} \cdot \boldsymbol{e}_{m(\boldsymbol{r})}(\boldsymbol{r})\delta_{1\tau(m(\boldsymbol{r}))}$$
$$+ \boldsymbol{p}_{m(\boldsymbol{r}')} \cdot \boldsymbol{e}_{m(\boldsymbol{r}')}(\boldsymbol{r}')\delta_{1\tau(m(\boldsymbol{r}'))} \big) \big], \quad (3)$$

which expresses the heterophilic cell-cell adhesion on the interface between the leader cells and follower cells. γ_H is the strength of surface tension and γ_p is the polarized component of the heterophilic adhesion [22,23]. $\boldsymbol{e}_m(\boldsymbol{r})$ is a unit vector indicating from $\boldsymbol{R}_m$ to $\boldsymbol{r}$, where $\boldsymbol{R}_m$ is the center of the mth cell as a parameter of adhesion molecule density [24]. The unit vector $\boldsymbol{p}_m$ that is the adhesion polarity of the mth cell,

$$\frac{d\boldsymbol{p}_m}{dt} = \nu \left[\frac{d\boldsymbol{R}_m}{dt} - \left(\frac{d\boldsymbol{R}_m}{dt} \cdot \boldsymbol{p}_m \right) \boldsymbol{p}_m \right]. \qquad (4)$$

The equation indicates the dynamics of $\boldsymbol{p}_m$ following the polarity of cytoskeletal polarization in the direction of $d\boldsymbol{R}_m/dt$ [25] and, furthermore, the adhesion molecules binding with intracell cytoskeletons, which is well known [26]. This term results in the driving force of leader cell motions in the direction of $\boldsymbol{p}_m$ [27]. Note that the driving is exerted

only through the contact with follower cells [21]. Here, ν is the ratio of $d\boldsymbol{p}_m/dt$ to $d\boldsymbol{R}_m/dt$. $\boldsymbol{R}_m$ is quasistatically equal to the center of domain mass $\sum_{\boldsymbol{r}} \boldsymbol{r}\delta_{mm(\boldsymbol{r})}/A_m$ with $A_m = \sum_{\boldsymbol{r}} \delta_{mm(\boldsymbol{r})}$.

The third term in the RHS of Eq. (1) is the bulk term,

$$\mathcal{H}_B = \kappa A \sum_m (1 - \frac{A_m}{A})^2, \qquad (5)$$

which maintains areas of cells to A. Here κ is the bulk modulus and A is the reference area. These values are independent of m and therefore $\tau(m)$.

On the basis of $\mathcal{H}$, we simulate the cell dynamics by the following Monte Carlo simulation [20]: The time unit of this simulation is taken to be a single Monte Carlo step (MCs). In this unit, L^2 single flips are attempted. The flip indicates the copy trial of a Potts state from a randomly chosen site $\boldsymbol{r}$ to its randomly chosen nearest or next nearest sites. The flip is accepted with the Metropolis probability $\min\{1, \exp[-\beta(\mathcal{H}_c - \mathcal{H})]\}$ with the Hamiltonian of the copied state, $\mathcal{H}_c$. After this procedure in MCs, $\boldsymbol{p}_m$ is updated once by Eq. (4) and $\boldsymbol{R}_m$ is set to the center of domain mass, respectively.

3   Simulations

At the beginning of this section, we explain the system used in the simulation. We impose the periodic boundary condition for simplicity on the analysis of the cell motion. For avoiding a finite size effect of a boundary condition, we employ a sufficiently large system with $L = 192$. For the purpose of checking the effect of the leader cells, we compare two cases. The first system consists of 32 followers and 32 leaders and the second system consists of 56 followers and 8 leaders. For convenience, we call the former the dense leader case and call the latter, the sparse leader case. The latter case corresponds to the expected situation for the rotation in the introduction.

Next, we move onto the explanation of the model parameters. We consider the parameters $\beta = 0.5$, $\kappa = 10$, $\tau = 10$ to realize the cell motion by the flexible deformations of cell shapes. For realizing the collective motion of cells, the aggregation of all the cells are necessary [1]. For this, we set surface tensions between cells less than twice the cell-empty interface tensions. Concretely, we impose $\gamma_C^2 = \gamma_H = 4.0$ and $\gamma_E^1 = \gamma_E^2 = 6.0$. For this, we set $\gamma_C^1 = 9.0$ larger than $2\gamma_H$. We also assume the leader cells aggregate without follower cells, and therefore impose γ_C^1 less than $2\gamma_E^1$. For the propulsion, we employ a sufficiently large value of γ_p, 1.0. By this choice, we can easily observe the motions of leader cells in cell aggregations and satisfy a necessary condition for the leader to drag the follower cell rotations.

In these settings, we simulate the collective motion of cells. Hereafter, we explain the simulation and the observations of the collective motion. From Eq. 4, the collective motion is expected to reflect in
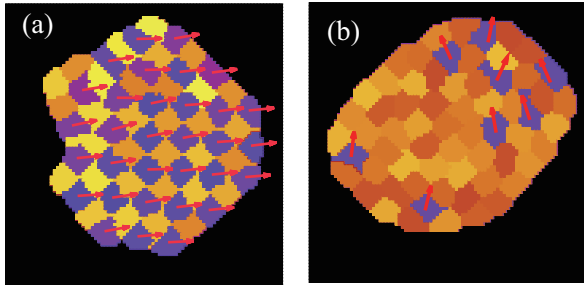
Fig. 1: Snapshots of cell configurations for (a) the dense leader case and (b) the sparse leader case. Violet colored domains are leader cells. Yellow or orange colored domains are follower cells. Red arrows in leader domains represent the direction of adhesion polarity.
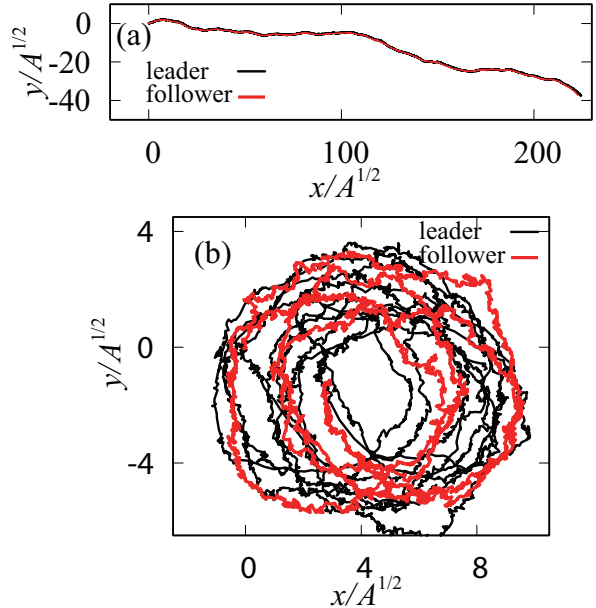

Fig. 2: Trajectories of a leader cell and a follower cell for (a) the dense leader case and (b) the sparse leader case. Black line represents the trajectory of a leader cell. Red line represents the trajectory of a follower cell. The origin of trajectories is taken at the position of the follower after the relaxation.

the configuration of leaders' polarities. Therefore, to confirm the type of collective cell motion, we sample cell polarities in the steady states. In this case, the initial state consists of an 8-by-8 array of cells. Each cell has the 8-sites × 8-sites square shape and they are separated from the neighboring cells by an interval. The leader cells are aligned at 4-by-8 for the dense leader case and 1-by-8 for the sparse leader cells. In this case, the leader cells are separated from the follower cells. To obtain the steady states from this initial state, we simulate the relaxation of the state during 2×10^4 MCs. After the relaxation, we sample steady states. The steady states do not depend on the initial states. In fact, the leader and follower cells mix as shown in Fig. 1 and therefore relax their surface tension from the initially-separated states. Here, the panels (a) and (b) show the aggregated state of cells for the dense and sparse leader cases, respectively.

For the dense leader case, the leader configuration takes a checkerboard pattern of leader cells [28, 29]. This pattern reflects the suspension condition of leader cells in the aggregation: The surface tensions satisfy $2\gamma_H < \gamma_C^1$ and inhibits the contacts between the leader cells. Owing to this pattern, the leader cells are relatively restricted to each other in their relative positions. This restriction effectively realizes a similar situation of a uniform system consisting of leaders and reflects in the unidirectional polarity order of leader cells. As a result, the cell aggregation behaves as a moving droplet with motility persistence.

In contrast to the dense leader case, the leader cells in the sparse leader case randomly disperse in the aggregation of cells. The random dispersion results from the absence of the positional restriction and thereby the disorder of the leader polarities. However, the polarities in the snapshot seemingly rather align in similar directions in contrast to the rotation in the contact following [6]. Therefore, if the collective rotation appears, the rotation may not steadily but statistically occur in a long time

even if it occurs. For the careful examination of the rotation, the cell rotation should be confirmed not indirectly by the snapshot but directly by the trajectories of cells.

To directly confirm the cell rotation from the cell trajectories, we calculate the trajectories of the leader and follower cells. For the comparison with the dense leader case with the polar order, we show the trajectories in Fig. 2(a) for the dense leader case and in Fig. 2(b) in the sparse leader case. For the dense leader case, the trajectories of the leader and follower cells are almost the same and therefore, suggest the collective cell motion in the same direction. In contrast to this, the rotational motion of the cells appears in the sparse leader case as previously expected. Thus, we confirm the collective cell rotations as a leader effect.

To speculate the driving mechanism of this rotation, we focus on the leader motion in this rotation. Leader cells mainly stay in the boundary of aggregation and move along it in our observation. In fact, reflecting this motion, the leaders take their rotation radius equal to the radius of the aggregations, which is $(NA/\pi)^{1/2} \sim 4.5A^{1/2}$ as shown in Fig. 2(b). From this observation, we can speculate that the leaders drive the boundary of the aggregation in the rotation direction by dragging follower cells because the leader cells cannot move in the normal direction of the boundary.

4 Summary and Remarks

In conclusion, we confirm the collective cell rotation guided by leader cells. From our simulation, the number of leader cells is necessary to be small for stabilizing the rotation. This is because the dense leader cells stabilize the polar order and thereby inhibit the rotation [19].

This collective cell rotation has two prominent properties. One prominent property is the persistence of the collective cell rotation. Namely, the direction of the rotation does not change in a long time. The mechanism of this persistence may originate from the persistence of leaders' polarities. However, as shown in Fig. 1(b), the direction of leaders' polarities are not always aligned in the same direction consistent with the rotation. Namely, the persistence of polarities apparently does not contribute to the persistence of the rotation. Therefore, another origin of the persistence of rotation is expected. One possibility of this alignment is the long-range coupling of leaders' polarities through the motion of follower cells as shown by Kabla for the collective migration [19]. This coupling may statistically stabilize a slight net polarity consistent with the rotation.

The other prominent property is the fact that the velocities of leader cells are two times faster than those of follower cells as shown in the number of trajectory circles in Fig. 2(b). This property may be useful as a sufficient marker of the leader-guiding. Namely, the leader mechanism can be explored by the experimental observation of the cell trajectories in the collective cell rotation in the future. When our setting is realized, the distribution of cell velocity or displacement is predicted to become bimodal because of the difference between the leader and follower cells in their velocities. Such a bimodal distribution has never been reported in experiments of *Dictyostelium discoidem* at least. Therefore, this absence of the report at least in *Dictyostelium discoidem* implies another still-uncovered solution where the leader and follower have the same velocity.

For the universality of these properties on the propulsion, we additionally give a remark. In the present work, we assume the heterophilic cell-cell adhesion as a propulsion source of leader cells. We expect that these properties do not depend on the origin of the motility and depend only on the persistence of motility's polarity. This is necessary for rotations of leaders to avoid simple random walks. If the polarity has persistence, this leader mechanism is applicable to the cases of propulsion by either chemotaxis or molecular chirality.

5 Acknowledgement

References

[1] P. Friedl and D. Gilmour, Nature Rev. Mol. Cell Bio. **10**, 445 (2009)

[2] G. E. Holloway *et al.*, Dev. Cell 12, 207 (2007).

[3] J. T. Bonner, *The Social Amoebae: The Biology of Cellular Slime Molds* (Princeton University Press, 2008).

[4] Here, the word "spontaneous" means the exclusion of the rotations due to the artificial confinement.

[5] A. Nicol *et al.*, J. Cell Sci. **112**, 3923 (1999).

[6] W.-J. Rappel et al., Phys. Rev. Lett. 83, 1247 (1999).

[7] T. Umeda and K. Inouye, J. theor. Biol. 219, 301 (2002).

[8] A. Tamada and M. Igarashi, Nat. Comm. **8**, 2194 (2017).

[9] H. Takagi, M. J. Sato, T. Yanagida, and M. Ueda: PLOS One3(2008)e2648.

[10] L. Li, E. C. Cox, and H. Flyvbjerg: Phys. Biol.8(2011) 046006.

[11] C. A. Weber et al., Phys. Rev. Lett.110(2013) 208001.

[12] T. Hanke, C. A. Weber, and E. Frey, Phys. Rev. E **88**, 052309 (2013).

[13] T. Hiraoka, T. Shimada, and N. Ito, Phys. Rev. E 94, 062612 (2016).

[14] K. Matsushita, K. Horibe, N. Kamamoto, K. Fujimoto, J. Phys. Soc. Jpn. **88**, 103801 (2019).

[15] K. Matsushita, K. Horibe, N. Kamamoto, S. Yabunaka, and K. Fujimoto, Proc. Sympo. Simul. Traffic Flow **25**, 21 (2019).

[16] M. Akiyama *et al.*, Develop. Growth Differ. **59**, 471 (2017).

[17] M. Hayakawa *et al.* eLife **9**, e53609 (2020).

[18] T. Vicsek *et al*, Phys. Rev. Lett. **75**, 1226 (1995).

[19] A. J. Kabla, J. R. Soc. Interface **9**, 3268 (2012).

[20] F. Graner and J. A. Glazier, Phys. Rev. Lett. **69**, 2013 (1992).

[21] K. Matsuashita, Phys. Rev. E **101**, 052410 (2020).

[22] J. C. Coates & A. J. Wood. J. Cell Sci. **114**, 4349 (2001).

[23] H. Sesaki & C. H. Siu, Dev. Biol. **177**, 504 (1996).

[24] K. Matsushita, Phys. Rev. E **95**, 032415 (2017).

[25] B. Szabó, G. J. Szollosi, B. Gonci, Z. Juranyi, D. Selmeczi, and T. Vicsek: Phys. Rev. E, **74** 061908 (2006).

[26] J Hülsken, W Birchmeier, J Behrens, J. Cell Biol. **127**, 2061 (1994).

[27] K. Matsushita, Phys. Rev. E **97**, 042413 (2018).

[28] H. Honda, H. Yamanaka, and G. Eguchi, J. Embryol. Exp. Morph. **98**, 1 (1986).

[29] J. A. Glazier and F. Graner, Phys. Rev. E 47, 2128 (1993).

E-mail: kmatsu@bio.sci.osaka-u.ac.jp